

Supporting Information

Elucidating Mechanism of Microscopic Conduction in Cathode Composites for All-Solid-State Batteries through Scanning Spreading Resistance Microscopy

Hirotsada Gamo, Yasushi Maeda,* Tetsu Kiyobayashi, Zyun Siroma, and Hikaru Sano

Contents

Fabrication of NCM pellets for SSRM	1
Verification of the SSRM simulator	2
Figure S1. Current–time curves in DC measurements for (a) 66NMC-34SE, (b) 45NMC-55SE, (c) 34NCM-66SE, and (d) 22NMC-78SE cathode composites. (e) Response current plotted as a function of applied voltage in NCM-SE cathode composites.	3
Figure S2. (a) Local resistance mapping and (b) resistance histogram of an NCM pellet without SE.	4
Figure S3. Schematic of 3D volume data in the simulation of (a) direct-current conductivity test and (b) SSRM measurement. Mean values of the non-zero current values in a plane slice parallel to the insulating layer is plotted as functions of depth (distance from the surface). Insulating layers with conductive windows of pixel sizes (c) 64×64 and (d) 1×1 are shown.	5
Figure S4. 3D structure models generated by SliceGAN for NCM-SE cathode composites with ratios of 66/34, 45/55, 34/66, and 22/78.	6
Figure S5. (a) Effective electronic conductivities and (b) the volume fraction of isolated NCM in NCM particles as functions of NCM volume fractions in the 3D volume data of the NCM-SE cathode composites. These properties have been calculated using the Taufactor program. ¹	8
Figure S6. Current density mapping of transport pathways via NCM particles with (a) low and (b) high resistances in the 3D volume data of the 45NCM-55SE cathode composite.	9
References	10

Fabrication of NCM pellets for SSRM

NCM powder (80 mg) was filled into a cylinder containing two stainless-steel rods, followed by uniaxial pressure of 360 MPa at room temperature to fabricate an NCM pellet with a diameter of approximately 10 mm. The resulting NCM pellet was then dipped in epoxy resin and heated at 60 °C for 3 h to obtain the NCM pellet for SSRM.

Verification of the SSRM simulator

To validate the developed SSRM simulation program, the program was executed on volume data (64^3 voxel size) with a conductivity of 1 (dimensionless) in each voxel. An insulating layer with conductive windows, featuring pixel sizes of 64×64 and 1×1 , was employed to replicate the direct-current conductivity test and SSRM measurement, respectively. Figure S3 illustrates the mean current values in a plane slice parallel to the insulating layer as a function of the depth from the surface where the conductive window is positioned.

In the simulation employing a conductive window (64×64 pixels), the electric field gradient and current density remained constant. In contrast, the SSRM simulation using a conductive window (1×1 pixel) revealed the voltage breakdown in the voxel near the window location. This behavior corresponds to the observation that a strong electric field below the probe leads to voltage breakdown in the SSRM observations. These results indicated that the developed program operates well as an SSRM simulator.

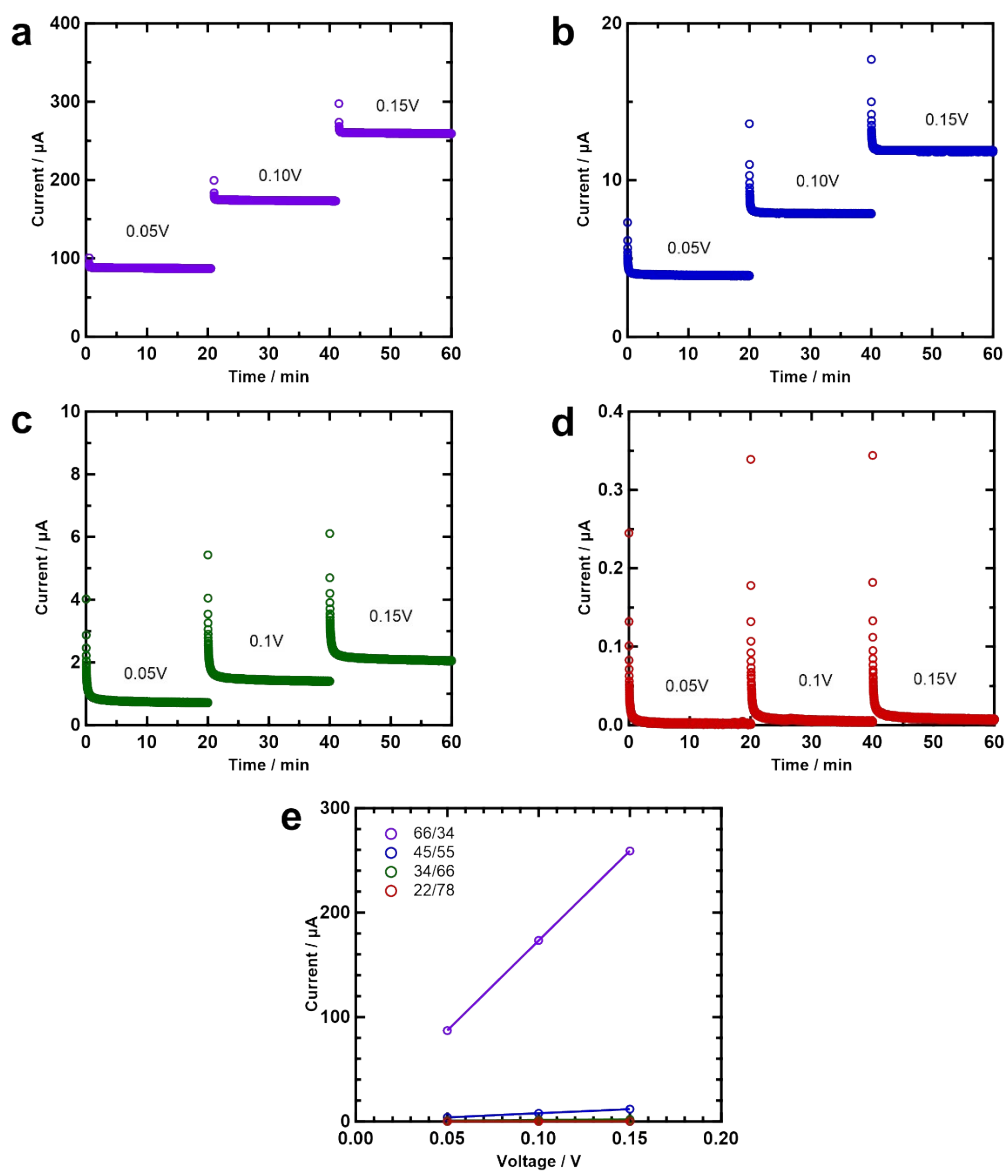


Figure S1. Current–time curves in DC measurements for (a) 66NMC-34SE, (b) 45NMC-55SE, (c) 34NCM-66SE, and (d) 22NMC-78SE cathode composites. (e) Response current plotted as a function of applied voltage in NCM-SE cathode composites.

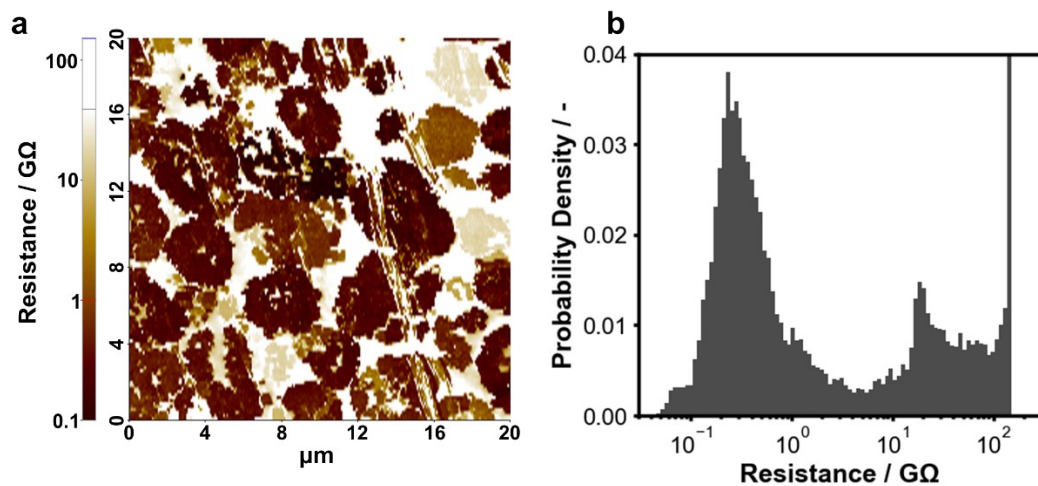


Figure S2. (a) Local resistance mapping and (b) resistance histogram of an NCM pellet without SE.

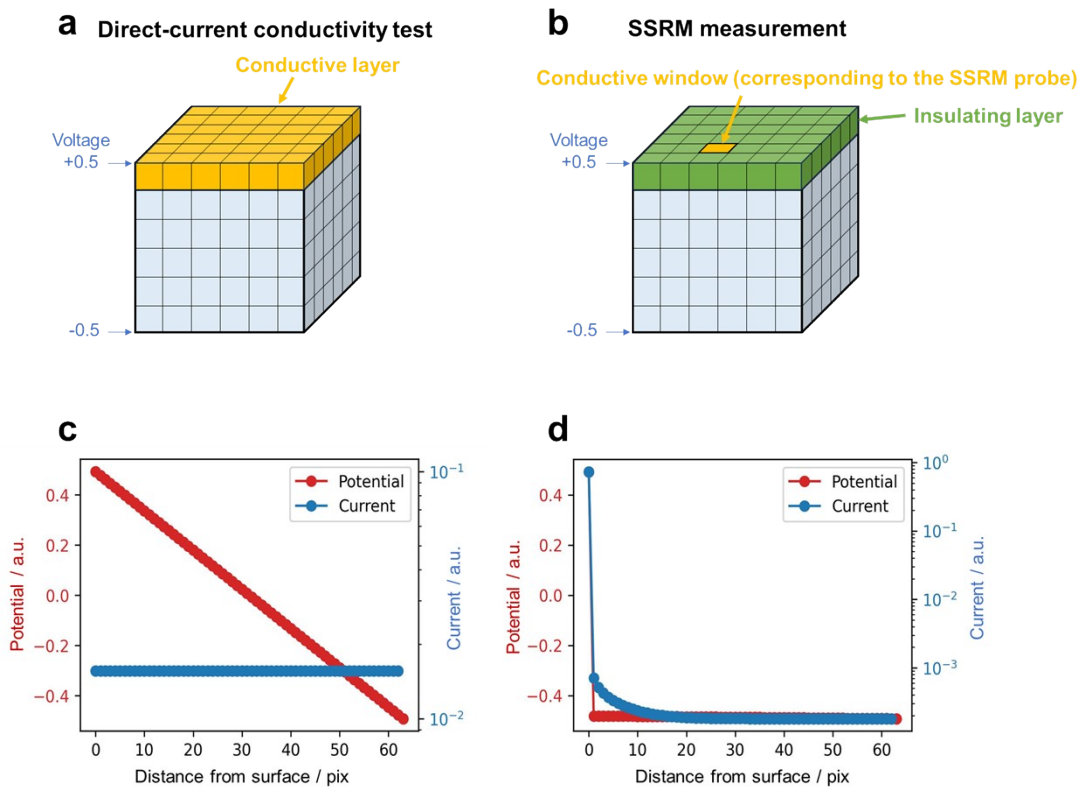


Figure S3. (a,b) Schematic of 64^3 volume for the simulation of direct-current conductivity test and SSRM measurement. (a) With a conductive layer. (b) With an insulating layer containing the conductive windows of pixel size 1×1 . (c,d) Mean values of the non-zero current component in a plane slice parallel to the top layer plotted as functions of depth (distance from the surface). (c) correspond to (a) and (d) corresponds to (b).

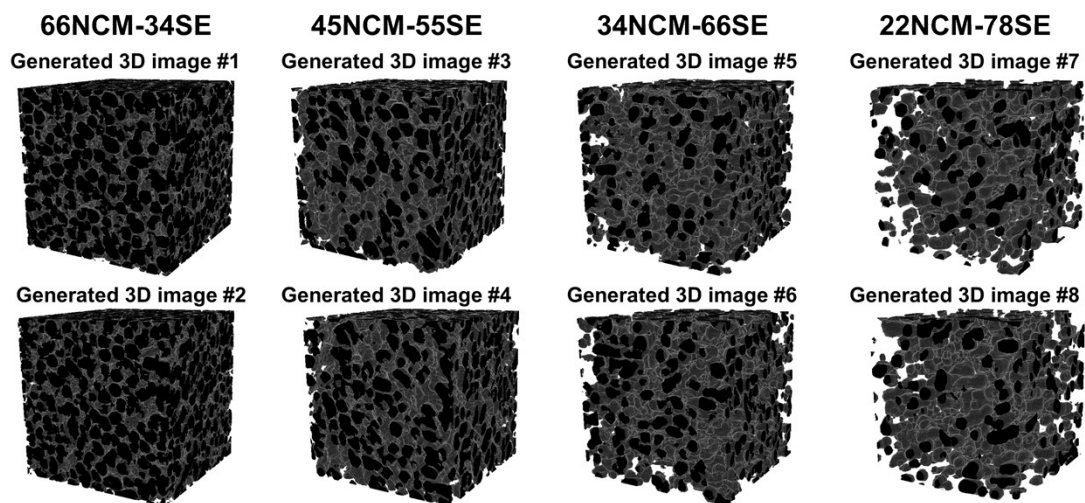


Figure S4. 3D structure models generated by SliceGAN for NCM-SE cathode composites with ratios of 66/34, 45/55, 34/66, and 22/78.

Table S1. 2D microstructural properties obtained from the original image.

Sample	Original SEM image			
	Area fraction (%)	Perimeter (μm)	Circularity	Particle density (μm^{-2})
66NCM-34SE	66.1	18	0.712	0.04
45SEM-55SE	44.8	14.1	0.674	0.042
34NCM-66SE	35.5	11.9	0.698	0.040
22NCM-78SE	22.9	11	0.795	0.025

Table S2. Average values of the 2D microstructural properties calculated from each slice in the generative 3D volume data.

Composition	Sample	3D volume data generated by SliceGAN			
		Volume fraction (%)	Perimeter (μm)	Circularity	Particle density (μm^{-2})
66NCM-34SE	Display in Fig.4	66.0	18.4	0.739	0.042
66NCM-34SE	Generated 3D image #1	66.4	12.9	0.810	0.061
66NCM-34SE	Generated 3D image #2	66.6	12.9	0.810	0.060
45SEM-55SE	Display in Fig.4	46.6	15.4	0.647	0.042
45SEM-55SE	Generated 3D image #3	47.7	12.6	0.669	0.051
45SEM-55SE	Generated 3D image #4	46.6	12.4	0.673	0.052
34NCM-66SE	Display in Fig.4	32.2	10.6	0.699	0.050
34NCM-66SE	Generated 3D image #5	33.9	8.1	0.740	0.062
34NCM-66SE	Generated 3D image #6	34.4	8.4	0.730	0.06
22NCM-78SE	Display in Fig.4	22.4	9.9	0.712	0.031
22NCM-78SE	Generated 3D image #7	21.9	9.9	0.713	0.030
22NCM-78SE	Generated 3D image #8	23.8	10.2	0.704	0.031

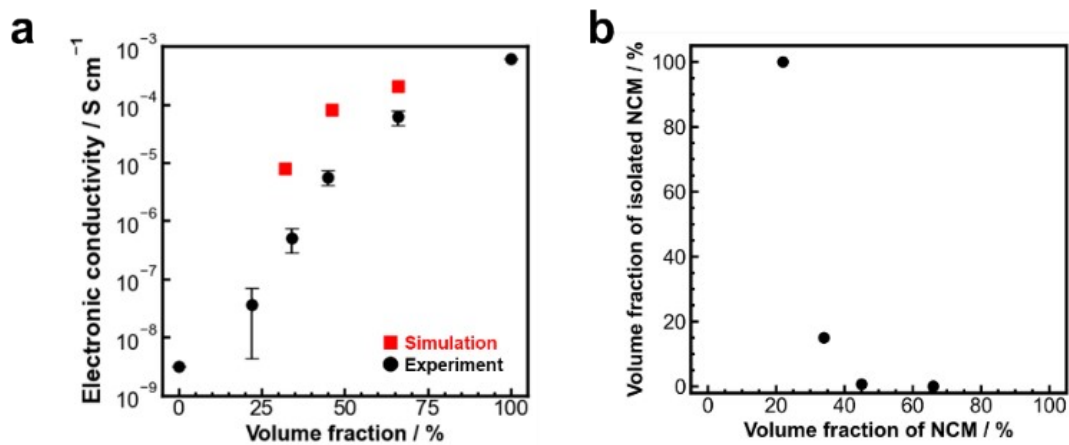


Figure S5. (a) Effective electronic conductivities and (b) the volume fraction of isolated NCM in NCM particles as functions of NCM volume fractions in the 3D volume data of the NCM-SE cathode composites. These properties have been calculated using the Taufactor program.¹

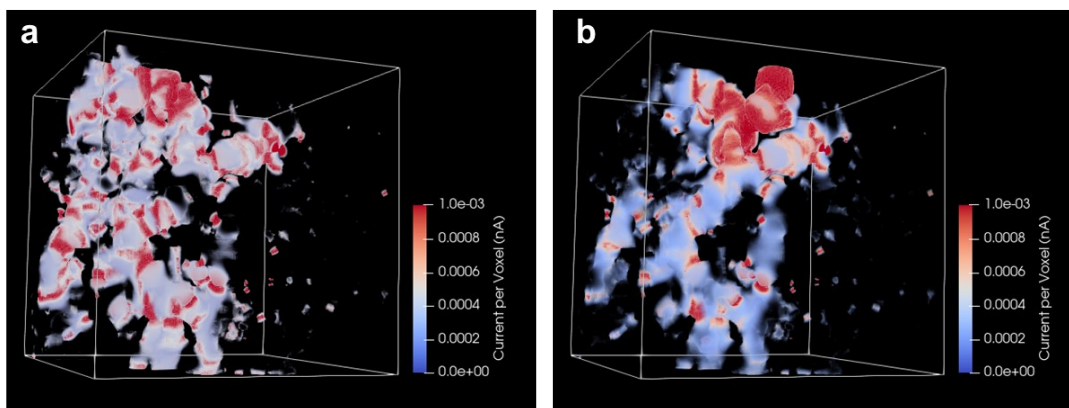


Figure S6. Current density mapping of transport pathways via NCM particles with (a) low and (b) high resistances in the 3D volume data of the 45NCM-55SE cathode composite.

References

- [1] S. J. Cooper, A. Bertei, P. R. Shearing, J. A. Kilner and N. P. Brandon, *SoftwareX*, 2016, 5, 203–210.